Letter

Complete delocalization and reentrant topological transition in a non-Hermitian quasiperiodic lattice

Ashirbad Padhan, Soumya Ranjan Padhi, and Tapan Mishra*

School of Physical Sciences, National Institute of Science Education and Research, Jatni 752050, India and Homi Bhabha National Institute, Training School Complex, Anushaktinagar, Mumbai 400094, India

(Received 28 July 2023; accepted 4 January 2024; published 19 January 2024)

We predict a complete delocalization of the localized states following the localization transition in a one-dimensional non-Hermitian Aubry-André model with a generalized quasiperiodic potential. We show that the system first undergoes a transition from the delocalized phase to the localized phase and then to the delocalized phase as a function of the complex phase of the quasiperiodic potential of fixed strength revealing a reentrant delocalization transition. We further identify the localized region as topological in nature exhibiting a well-defined spectral winding number which vanishes in the delocalized phases resulting in a reentrant spectral topological transition. Moreover, we find that these two transitions occur through intermediate regions hosting both delocalized and localized states which also possess nontrivial winding numbers that are different from that of the localized phase.

DOI: 10.1103/PhysRevB.109.L020203

Introduction. The quasiperiodic lattices which are intermediate to periodic and random lattices have enriched our understanding on the localization transition [1]. One of the striking features of such lattices is the well-defined localization transition in one dimension as opposed to their random counterparts where the localization of states occurs for any infinitesimal strength of disorder. The simplest quasiperiodic lattice model is the paradigmatic Aubry-André (AA) model which exhibits a sharp delocalization-localization (DL) transition of the single particle states at a critical quasiperiodic potential strength owing to the self-duality of the model [2,3]. However, generalization of the AA model results in the localization transition through an intermediate phase with coexisting localized and delocalized states separated by critical energies known as the mobility edge [4–11]. However, the studies on the non-Hermitian generalizations of the AA model and its variants have predicted interesting scenarios such as sharp DL transitions, associated parity-time ($\mathcal{PT}$) symmetry breaking, butterfly spectra, non-Hermitian mobility edges, appearance of topological edge states, etc. [12–25]. Recent studies have also found the DL transition in nHAA model as a topological phase transition by associating the localized spectrum with a spectral winding number [26–29].

Until recently it was believed that in the DL transitions once the states are localized they remain localized as a function of the disorder strength or other parameters. However, the prediction of the reentrant localization transition in certain dimerized quasiperiodic chains by some of us [30,31] has brought in a renewed interest in the field of localization transitions. This counterintuitive phenomenon involves a partial delocalization of the localized spectrum (or delocalization of some of the localized states) after the system has undergone a localization transition and has been predicted in numerous Hermitian and non-Hermitian systems [32–38] leading to their recent experimental realizations [39,40].

While the studies reported so far involve the delocalization of some of the localized states or partial delocalization of the spectrum as a function of the disorder or other system parameters, in this paper we predict a complete delocalization of the localized spectrum in a parameter regime of the model. We show that in the case of a non-Hermitian generalized AA model the system after undergoing a DL transition returns to the delocalized phase as a function of the complex phase in the quasiperiodic potential. We term this nature of the transition starting from a delocalized phase and then returning back to another delocalized phase as a *reentrant* delocalization transition. Moreover, we find that the localized phase possesses a nontrivial spectral winding number which vanishes in the delocalized phases resulting in a reentrant topological phase transition as a function of the complex phase. We also find that the DL and LD transitions occur through the intermediate phases having coexisting delocalized and localized states which are also found to be of topological in nature. In the following we discuss these findings in detail.

Model. The non-Hermitian generalized AA (nHGAA) model is defined as

$$H = -J\sum_{n=1}^{L}(c_n^\dagger c_{n+1} + \text{H.c.}) + \lambda\sum_{n=1}^{L}\frac{\cos(2\pi\beta n+\phi)}{1-\alpha\cos(2\pi\beta n+\phi)}c_n^\dagger c_n, \tag{1}$$

where $c_n^\dagger(c_n)$ is the creation (annihilation) operator of spinless fermions at the nth lattice site. J is the nearest-neighbor hopping amplitude and λ represents the strength of the quasiperiodic potential. Here $\beta = (\sqrt{5}-1)/2$—an irrational

*mishratapan@niser.ac.in

number known as the inverse golden ratio. We introduce non-Hermiticity by writing $\phi = \theta + ih$. Note that the model is $\mathcal{PT}$ symmetric if we choose $\theta = 0$ [20]. Therefore, we consider $\theta = 0$ throughout unless otherwise mentioned.

For $\alpha = 0$ and $h = 0$, the model in Eq. (1) reduces to the Hermitian AA model that exhibits a DL transition of the entire spectrum at $\lambda = 2J$ due to the self-duality of the model [2]. However, when h is finite, the model is non-Hermitian and is shown to undergo a DL transition at a critical $h = \ln(2J/\lambda)$ in Ref. [26]. Also after this critical h, all the real eigenenergies become complex (a real-complex transition), indicating a $\mathcal{PT}$ symmetry-breaking phase transition in the system. Due to the presence of the complex energy spectrum, the localized phase is found to possess nontrivial spectral winding number and hence a trivial to topological transition at the DL transition. In our study, we show that when α becomes finite, a completely different scenario appears where the system undergoes a delocalization-localization-delocalization (DLD)-type transition which we further characterize as a trivial-topological-trivial transition based on the spectral winding numbers. These findings are obtained by numerically solving the model shown in Eq. (1) using the exact diagonalization method under periodic boundary conditions (PBCs) with systems of size up to $L = 6765$. We set $J = 1$ as the energy scale and fix the strength of the quasiperiodic potential $\lambda = 1$.

In the following, we discuss our findings in detail. First we will focus on the DL transition in the system. Next we will investigate the spectral topological character associated to these transitions.

Delocalization-localization transition. We begin our discussion by identifying the delocalized and localized regions in the α-h plane as depicted in Fig. 1(a). The regions in the left and right sides of the boundaries marked with green squares and white circles respectively correspond to delocalized phases (D) and the region below the yellow triangles corresponds to the localized phase (L). The white central region enclosed by these three lines is the intermediate phase (I) where both delocalized and localized states coexist. These boundaries are obtained from the inverse participation ratio (IPR), given by $\text{IPR}_n = \sum_{j=1}^{L} |\psi_n^j|^4$ and the corresponding normalized participation ratio (NPR) given by $\text{NPR}_n = 1/(L \times \text{IPR}_n)$ [28,41] with ψ_n^j as the nth eigenstate of the Hamiltonian shown in Eq. (1). The IPR (NPR) takes vanishing (finite) and finite (vanishing) value for a delocalized and a localized state, respectively for a finite system. However, to obtain the insight about the entire spectrum, we utilize $\langle \text{IPR} \rangle$ and $\langle \text{NPR} \rangle$ where $\langle \cdot \rangle$ stands for the average over all eigenstates. In Fig. 1(d), we plot $\langle \text{IPR} \rangle$ (red solid line) and $\langle \text{NPR} \rangle$ (blue dashed line) as a function of h for an exemplary value of $\alpha = 0.2$ [white dashed line in Fig. 1(a)]. The values of $\langle \text{IPR} \rangle = 0$ and $\langle \text{NPR} \rangle \neq 0$ in the regions $h \lesssim 0.325$ and $h \gtrsim 4.25$ [light blue regions in Fig. 1(d)] indicate that all the states in the system are delocalized. In the range $1.35 \lesssim h \lesssim 3.25$ (light red region), the states are localized which is indicated from the values $\langle \text{IPR} \rangle \neq 0$ and $\langle \text{NPR} \rangle = 0$. However, there exist two intermediate regions on either sides of the localized region where both $\langle \text{IPR} \rangle$ and $\langle \text{NPR} \rangle$ remain finite [white regions between $0.325 \lesssim h \lesssim 1.35$ and $3.25 \lesssim h \lesssim 4.25$ in Fig. 1(d)]. The boundaries in the phase diagram shown in Fig. 1(a) are obtained by plotting the average participation ratios at different values of α. The different phases are further analyzed by looking at the individual eigenstates in Figs. 1(b) and 1(c) where we plot the IPR values as a function of eigenvalues and h. In the delocalized (localized) phase all the states are delocalized (localized). However, both delocalized and localized states coexist in the intermediate phases. Moreover, the delocalized and localized states are separated by critical energies known as the mobility edge.

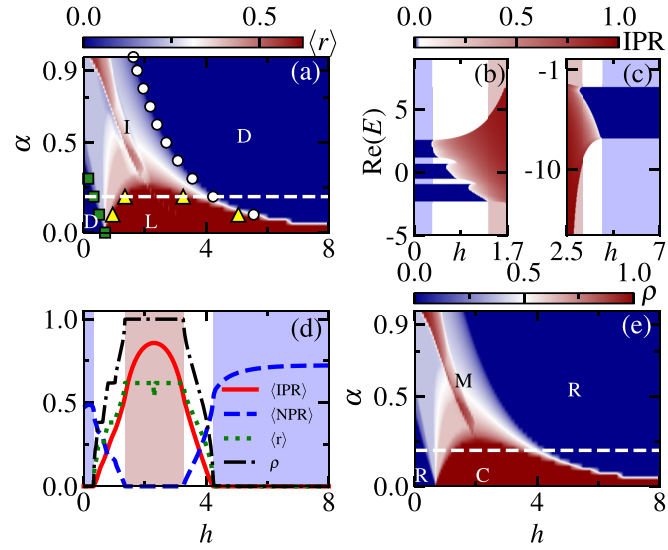

FIG. 1. (a) The phase diagram in the α-h plane, obtained using the average inverse participation ratio ($\langle \text{IPR} \rangle$) and average normalized particpation ratio ($\langle \text{NPR} \rangle$) values indicating the delocalized (D), intermediate (I), and localized (L) phases. The color code indicates the values of average adjacent gap ratio ($\langle r \rangle$) superimposed in the figure. (b) and (c) show the IPR plotted as a function of the real energy eigenvalues and h. (d) $\langle \text{IPR} \rangle$ (red solid line), $\langle \text{NPR} \rangle$ (blue dashed line), $\langle r \rangle$ (green dotted line) and ρ (black dashed-dotted line) are plotted as a function of h for $\alpha = 0.2$ that corresponds to the white dashed line in panels (a) and (e) indicating a delocalization-localization-delocalization (DLD) and real-complex-real (RCR) transition. (e) The phase diagram in the α-h plane obtained using the values of density of states (ρ) which distinguishes the real (R), mixed (M), and complex (C) phases. For the figures in panels (b) and (c) a system of length $L = 2584$ is considered and $L = 6765$ is considered for panels (a), (d), and (e).

It can be noticed from the phase diagram that when $\alpha = 0$, a sharp DL transition occurs at $h = \ln(2J/\lambda)$—a feature already predicted in Ref. [26]. However, when α becomes finite, a DLD transition occurs as a function of h where a complete delocalization of the localized states occur indicating a reentrant delocalization transition for a range of values of α. Unlike the transition at $\alpha = 0$, these transitions occur through the intermediate regions and are not sharp. For $\alpha \gtrsim 0.25$, some of the delocalized states get localized resulting an intermediate phase and then a complete delocalization of the states occurs as h increases. For higher values of α, the complete delocalization of states occurs from an intermediate phase.

To further quantify this behavior, we compute the adjacent gap ratios (AGRs) defined by $r_n = \frac{\min(\epsilon_n, \epsilon_{n+1})}{\max(\epsilon_n, \epsilon_{n+1})}$ where $\epsilon_n = \text{Re}(E_{n+1}) - \text{Re}(E_n)$. Here the eigenvalues E_n are sorted in

ascending order according to their real parts only [34,41]. In Fig. 1(d), we plot the average AGR, i.e., $\langle r\rangle = \sum_n r_n/L$ (green dotted line) as a function of h for $\alpha = 0.2$. As expected, $\langle r\rangle$ vanishes in the delocalized phase and attains its maximum value in the localized phase but takes an intermediate value in the intermediate phase. To identify the phases from the behavior of $\langle r\rangle$ we plot $\langle r\rangle$ as a function of α and h in Fig. 1(a). The delocalized and localized regions can be clearly identified by the blue and red regions where $\langle r\rangle$ is zero and maximum respectively. This also matches well with the boundaries obtained from the average participation ratios [symbols in Fig. 1(a)]. The reason for the sharp dip in $\langle r\rangle$ at $h_c \sim 2.29$ inside the localized region will be discussed later.

The above analysis clearly shows that an increase in h leads to a complete delocalization of the localized states. For a range of α we also obtain a DLD-type reentrant delocalization transition where the transitions occur through intermediate phases. In the following our primary focus will be to understand this DLD transition from the eigenspectrum.

Analysis of the eigenspectrum. To analyze the spectrum in the current scenario, we examine the behavior of the density of states $\rho = N/L$, where N counts the number of states having complex eigenvalues in the spectrum and L is the system size. According to the definition, in the thermodynamic limit, ρ attains the value 0 (1) when none (all) of the eigenenergies are complex and the corresponding phase is $\mathcal{PT}$ unbroken (broken). To this end, we first plot ρ as a function of α and h in Fig. 1(e) which clearly depicts the regions of real energies (blue region) and complex energies (red region) where ρ becomes exactly zero and one respectively. We denote these regions with entire real and complex eigenenergies as R and C respectively. There also exists a region where the value of ρ is in between zero and one which indicates the presence of both real and complex eigenenergies in the spectrum and we call it the mixed (M) region. Note that similar to the phase diagram shown in Fig. 1(a), we also see a reentrant transition of type RCR in Fig. 1(e) for small values of α. This reentrant behavior can be seen from the plot of ρ as a function of h which is shown in Fig. 1(d) (white dashed line) for an exemplary cut through the phase diagram of Fig. 1(e) at $\alpha = 0.2$. From Fig. 1(d), we observe that initially $\rho = 0$, i.e., all the energies are real in the spectrum up to $h = 0.325$ (light blue region). As h increases, the value of ρ becomes finite and reaches its maximum, i.e., $\rho = 1$ in the range $1.35 < h < 3.25$ (light red region). In this range of h, the entire spectrum is complex and the states are localized. Further increase in h leads to a decrease in the value of ρ which eventually becomes zero for $h > 4.25$, after which the spectrum is real again (light blue region). This re-appearance of the entire real spectrum for large values of h is an indication of a reentrant RCR transition in the spectrum associated to a $\mathcal{PT}$ unbroken-broken-unbroken phase transition. The mixed regions are indicated by the white patches in Fig. 1(d) where ρ takes values between 0 and 1. Note that the step wise increase of ρ in the first mixed region is due to the gaps in the spectrum as shown in Fig. 1(b). Comparing the behavior of ρ with the participation ratios shown in Fig. 1(d), we obtain that the delocalized-intermediate-localized-intermediate-delocalized transitions of the eigenstates coincide with the real-mixed-complex-mixed-real transitions in the energies.

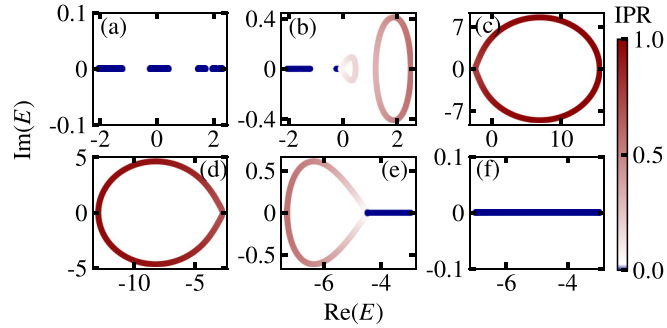

FIG. 2. [(a)–(f)] The IPR is plotted as a function of real and imaginary eigenvalues corresponding to $h = 0.2, 0.75, 2.0, 2.8, 3.75$, and 5.0, respectively, for $\alpha = 0.2$. Here a system of $L = 2584$ sites is considered.

We confirm this behavior by plotting the real and imaginary energies in Figs. 2(a)–2(f) for different values of h (i.e., $h = 0.2,\ 0.75,\ 2.0,\ 2.8,\ 3.75$, and 5.0). This shows that in the delocalized (localized) phase, all the energies are real (complex) as can be seen from Figs. 2(a) and 2(f). However, in the intermediate phases, both real and complex energies are present [see Figs. 2(b) and 2(e)]. Most importantly, when in the localized and intermediate phases, the presence of complex eigenvalues form loops as shown in Figs. 2(b)–2(e) for $h = 0.75,\ 2.0,\ 2.8,\ 3.75$, respectively, and we will show that these loops will characterise the topological nature of the phases.

Similar to the localization properties, the reentrant real-complex transition occurs for a small range of α. After $\alpha \gtrsim 0.25$, the spectrum is never entirely complex and the reentrant transition is of real-mixed-real type for $0.25 \lesssim \alpha \lesssim 0.375$ and for $\alpha \gtrsim 0.375$ the transition is of mixed-real type as can be seen from Fig. 1(e).

In the following, we will show that this appearance of reentrant RCR transition will reveal a much richer phenomenon in the context of spectral topology.

Reentrant topological transition. We will now identify the different phases with respect to their topological nature. To this end we compute the spectral winding number defined as [26,28,42]

$$w = \lim_{L\to\infty} \frac{1}{2\pi i} \int_0^{2\pi} d\theta \partial_\theta \log\left[\det\{H(\theta/L) - \varepsilon\}\right], \quad (2)$$

which in this case is the number of times the spectrum of H winds a base energy ε when the real θ varies from 0 to 2π. In the case of the nHAA model, there is a direct real-complex transition in the spectrum as a function of h, i.e., all the energies in the spectrum become complex after the transition. This relaxes the choice of the base energy which can be safely taken to be zero [26]. However, in the presence of the mobility edge between the delocalized and the localized states, the base energy can not be arbitrary due to the presence of the mixed states in the spectrum. In practice, two base energies are considered which correspond to the real energy eigenvalues that defines the beginning and the end of the intermediate or mixed region or the minimum and maximum energies on the mobility edge [28,29]. Following this prescription, we can identify the winding numbers across the DLD transition

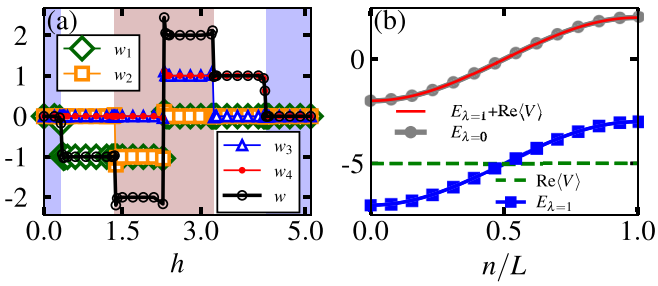

FIG. 3. Panel (a) shows the variation of spectral winding numbers w_1 (green diamonds), w_2 (orange boxes), w_3 (blue triangles), and w_4 (red filled circles) and total winding number w (black empty circles) as a function of h for $\alpha = 0.2$. The shaded blue (red) area denotes the trivial (nontrivial) phase. (b) Real eigenvalues for $\lambda = 0$ (gray line with dots), $\lambda = 1, h = 6.0$ (blue line with squares), its shifted energies (red solid line) and Re$\langle V\rangle$ (green dashed line) are plotted as a function of state index. Here the system size is considered to be $L = 233$ in panel (a) and $L = 2584$ in panel (b).

at smaller values of α, e.g., $\alpha = 0.2$ for which the DLD transition occurs through two intermediate or mixed regions resulting in four critical points.

In Fig. 2 we observed that the real versus imaginary eigenvalues form loops in the localized and intermediate phases. We link the winding numbers corresponding to these loops by identifying the base energies at the beginning and at the end points of the intermediate regions from the energy spectrum. For $\alpha = 0.2$, the base energies are $\varepsilon_1 \approx 2.274$ and $\varepsilon_2 \approx -2.042$ at the critical points h_1 and h_2 for D to I and I to L transitions, respectively. Similarly, we fix two other base energies across the second intermediate region, i.e., $\varepsilon_3 \approx -3.0$ and $\varepsilon_4 \approx -7.0$ at h_3 and h_4 are critical points for the L to I and I to D transitions, respectively. Accordingly, we obtain four winding numbers such as w_1 (green diamonds), w_2 (orange boxes), w_3 (blue triangles), and w_4 (red filled circles) using Eq. (2) which are plotted as a function of h in Fig. 3(a). We also plot the total winding number $w = w_1 + w_2 + w_3 + w_4$ (black circles) to clearly distinguish the different phases. As observed, all the winding numbers vanish in the delocalized phase due to the nonexistence of complex eigenvalues and this results in a reentrant topological transition. Apart from this we find that in the intermediate phase, one of the winding numbers is finite, (e.g., for $0.325 < h < 1.35$, $w_1 = -1$) and in the localized phase, two of them are finite (e.g., for $1.35 < h < h_c$, $w_1 = w_2 = -1$). However, a counterintuitive situation arises at h_c where the total winding number becomes nonquantized even though the system is in the localized phase. Moreover, at this point w changes its sign, i.e., when $h < h_c$, w is negative and when $h > h_c$, w is positive. Note that at h_c, a loop in the energy spectrum is expected since the system lies in localized phase at this point. However, as the largest eigenvalue is much larger compared to the other eigenvalues in the spectrum, a discontinuous loop is formed (not shown). This nature is also reflected in the value of $\langle r\rangle$ which decreases slightly from its maximum value of $\sim$0.6 [see Fig. 1(d)].

The reentrant phenomenon exhibited by the model is a result of the peculiar behavior of the disorder potential as a function of h. For small h, the disorder in the system is weak for which all the states are delocalized. As h is increased, the disorder in the system first increases, reaches a maximum and then decreases to a minimum value which is not sufficient to localize the states and hence we get a second delocalization transition. This complete delocalization can be understood by analyzing the energy spectrum of the system in the limit of large h. To provide an intuitive understanding, we consider $h = 6.0$ and plot the real eigenvalues as a function of state index in Fig. 3(b) (blue squares). This shows that the entire eigenspectrum is nothing but a continuum of extended or delocalized states—a situation similar to the case of zero or weak disorder, i.e., $\lambda \sim 0$ shown as red dots in Fig. 3(b). By comparing these two curves it is inferred that $E_{\lambda=1} = E_{\lambda=0} + C$ where C is a number. For $h = 6$, we obtain that $C = 5.0$ which can be observed from the complete overlap of $E_{\lambda=0} + 5.0$ curve (red solid line) and the $E_{\lambda=1}$ curve in Fig. 3(b). It turns out that the number C in this case is the expectation value of the onsite term of the Hamiltonian, i.e., $V = \lambda \sum_{n=1}^{L} V_n c_n^\dagger c_n$, where $V_n = \frac{\cos(2\pi\beta n+\phi)}{1-\alpha\cos(2\pi\beta n+\phi)}$, over all the eigenstates as shown in Fig. 3(b) (green dashed line).

This analysis reveals that as h becomes larger, the disorder potential in the system eventually vanishes and in this limit it tends to approach a constant value. This can be understood by rewriting the potential in the limit of large h as

$$V_n \to \frac{e^{-i(2\pi\beta n)}e^h/2}{1-\alpha e^{-i(2\pi\beta n)}e^h/2} \to -\frac{1}{\alpha}, \tag{3}$$

where $\cos(2\pi\beta n + ih)$ is written in terms of exponentials. With this we get a constant onsite potential of strength $-\lambda/\alpha = -5$ at all sites for $\lambda = 1$ and $\alpha = 0.2$. This is consistent with our numerical findings shown above.

Conclusions. We have predicted a phenomenon of complete delocalization of the spectrum after a localization transition and identified an associated reentrant topological transition as a function of the complex phase in a one-dimensional nHGAA model. We obtain that the reentrant topological transition is due to the real-complex-real transition in the eigenspectrum indicating a $\mathcal{PT}$ broken and subsequent unbroken phase transition. Moreover, we have also found that these transitions occur through two intermediate regions having both real and complex energy spectra and are topological in nature.

Our study reveals a counterintuitive scenario where the system returns to the metallic phase after undergoing a metal-insulator transition as a function of the Hermiticity breaking parameter in the quasiperiodic lattice for fixed disorder strength. This prediction will expand our scope to understand the localization transitions in quasiperiodic systems and in particular will provide possible new directions to explore the localization and topological physics in non-Hermitian systems. An immediate extension could be to ask the fate of such complete delocalization of the localized states in the presence of interaction. Another possibility will be to explore the transport properties in such models where nature

of transport can be studied while the system undergoes such reentrant transition. However, due to the recent progress in accessing quasiperiodic lattices in platforms such as photonic lattices [28], electrical circuits [20] and periodically driven systems [43] our prediction is in principle carries sufficient experimental relevance in the field.

Acknowledgments. We acknowledge fruitful discussions with S. D. Mahanti, Awadhesh Narayan, and M. J. Bhaseen. T.M. acknowledges support from Science and Engineering Research Board (SERB), Govt. of India, through Projects No. MTR/2022/000382 and No. STR/2022/000023.

[1] S. Aubry and G. André, Ann. Israel Phys. Soc. **3**, 18 (1980).
[2] G. A. Domínguez-Castro and R. Paredes, Eur. J. Phys. **40**, 045403 (2019).
[3] P. G. Harper, Proc. Phys. Soc. A **68**, 874 (1955).
[4] D.-L. Deng, S. Ganeshan, X. Li, R. Modak, S. Mukerjee, and J. H. Pixley, Ann. Phys. **529**, 1600399 (2017).
[5] X. Li and S. Das Sarma, Phys. Rev. B **101**, 064203 (2020).
[6] J. Biddle and S. Das Sarma, Phys. Rev. Lett. **104**, 070601 (2010).
[7] J. Biddle, D. J. Priour, B. Wang, and S. Das Sarma, Phys. Rev. B **83**, 075105 (2011).
[8] S. Ganeshan, J. H. Pixley, and S. Das Sarma, Phys. Rev. Lett. **114**, 146601 (2015).
[9] X. Li, X. Li, and S. Das Sarma, Phys. Rev. B **96**, 085119 (2017).
[10] H. Yao, A. Khoudli, L. Bresque, and L. Sanchez-Palencia, Phys. Rev. Lett. **123**, 070405 (2019).
[11] D. D. Vu and S. Das Sarma, Phys. Rev. B **107**, 224206 (2023).
[12] Q.-B. Zeng, Y.-B. Yang, and Y. Xu, Phys. Rev. B **101**, 020201(R) (2020).
[13] A. Jazaeri and I. I. Satija, Phys. Rev. E **63**, 036222 (2001).
[14] L.-Z. Tang, G.-Q. Zhang, L.-F. Zhang, and D.-W. Zhang, Phys. Rev. A **103**, 033325 (2021).
[15] X. Cai, Phys. Rev. B **103**, 014201 (2021).
[16] H. Jiang, L.-J. Lang, C. Yang, S.-L. Zhu, and S. Chen, Phys. Rev. B **100**, 054301 (2019).
[17] S. Longhi, Phys. Rev. B **103**, 054203 (2021).
[18] J. Claes and T. L. Hughes, Phys. Rev. B **103**, L140201 (2021).
[19] Q.-B. Zeng, S. Chen, and R. Lü, Phys. Rev. A **95**, 062118 (2017).
[20] Q.-B. Zeng and Y. Xu, Phys. Rev. Res. **2**, 033052 (2020).
[21] Y. Liu, Q. Zhou, and S. Chen, Phys. Rev. B **104**, 024201 (2021).
[22] S. Li, M. Li, Y. Gao, and P. Tong, Phys. Rev. B **105**, 104201 (2022).
[23] K. Kawabata, K. Shiozaki, M. Ueda, and M. Sato, Phys. Rev. X **9**, 041015 (2019).
[24] C. Yuce, Phys. Lett. A **378**, 2024 (2014).
[25] L.-J. Zhai, S. Yin, and G.-Y. Huang, Phys. Rev. B **102**, 064206 (2020).
[26] S. Longhi, Phys. Rev. Lett. **122**, 237601 (2019).
[27] S. Longhi, Phys. Rev. B **100**, 125157 (2019).
[28] T. Liu, H. Guo, Y. Pu, and S. Longhi, Phys. Rev. B **102**, 024205 (2020).
[29] L. Zhou and W. Han, Chin. Phys. B **30**, 100308 (2021).
[30] S. Roy, T. Mishra, B. Tanatar, and S. Basu, Phys. Rev. Lett. **126**, 106803 (2021).
[31] A. Padhan, M. K. Giri, S. Mondal, and T. Mishra, Phys. Rev. B **105**, L220201 (2022).
[32] Z.-W. Zuo and D. Kang, Phys. Rev. A **106**, 013305 (2022).
[33] S. Roy, S. Chattopadhyay, T. Mishra, and S. Basu, Phys. Rev. B **105**, 214203 (2022).
[34] W. Han and L. Zhou, Phys. Rev. B **105**, 054204 (2022).
[35] C. Wu, J. Fan, G. Chen, and S. Jia, New J. Phys. **23**, 123048 (2021).
[36] L. Zhou and W. Han, Phys. Rev. B **106**, 054307 (2022).
[37] R. Qi, J. Cao, and X.-P. Jiang, Phys. Rev. B **107**, 224201 (2023).
[38] H. Wang, X. Zheng, J. Chen, L. Xiao, S. Jia, and L. Zhang, Phys. Rev. B **107**, 075128 (2023).
[39] S. Vaidya, C. Jörg, K. Linn, M. Goh, and M. C. Rechtsman, Phys. Rev. Res. **5**, 033170 (2023).
[40] Z.-S. Xu, J. Gao, A. Iovan, I. M. Khaymovich, V. Zwiller, and A. W. Elshaari, arXiv:2307.05207.
[41] Y. Liu, X.-P. Jiang, J. Cao, and S. Chen, Phys. Rev. B **101**, 174205 (2020).
[42] Z. Gong, Y. Ashida, K. Kawabata, K. Takasan, S. Higashikawa, and M. Ueda, Phys. Rev. X **8**, 031079 (2018).
[43] S. Weidemann, M. Kremer, S. Longhi, and A. Szameit, Nature (London) **601**, 354 (2022).